NANO MICRO small

Graphene

Reduced Graphene Oxide Upconversion Nanoparticle Hybrid for Electrochemiluminescent Sensing of a Prognostic Indicator in Early-Stage Cancer

*Li Wu, Jiasi Wang, Meili Yin, Jinsong Ren, Daisuke Miyoshi, Naoki Sugimoto, and Xiaogang Qu**

Upconversion nanoparticles (UCNPs) have been proposed as a promising new class of biological luminescent labels because of their weak auto-fluorescence background, strong penetration ability under near-infrared (NIR) radiation, resistance to photobleaching, and low toxicity. Although UCNPs hold great promise in nanotechnology and nanomedicine, their applications in ECL fields still remain unexplored. Herein, a label-free, ultra-sensitive and selective electrochemiluminescence (ECL) assay is developed for detection of cyclin A_2 by using highly efficient ECL graphene-upconversion hybrid. Being an important member of the cyclin family, cyclin A_2 is involved in the initiation of DNA replication, transcription and cell cycle regulation through the association of cyclin-dependent kinases (CDK). Cyclin A_2 is a prognostic indicator in early-stage cancers and a target for treatment of different types of cancers. However, the expression level of cyclin A_2 is quite low, direct detection of cyclin A_2 in crude cancer cell extracts is challenging and important for both clinical diagnosis of cancer in the early stage and the treatment. By chemically grafting cyclin A_2 detection specific probe, a PEGlyted hexapeptide, to graphene-upconversion hybrid, the constructed ECL biosensor displays a superior performance for cyclin A_2, which can not only detect cyclin A_2 directly in cancer cell extracts, but also discriminate between normal cells and cancer cells. More importantly, the ECL biosensor has different responses between clinical used anticancer drug-treated and non-treated cancer cells, which demonstrates that the sensor can be potentially used for drug screening, and for evaluation of therapeutic treatments in early-stage cancers.

L. Wu, J. Wang, M. Yin, Prof. J. Ren, Prof. X. Qu
Laboratory of Chemical Biology
Division of Biological Inorganic Chemistry
State Key Laboratory of Rare Earth
Resource Utilization, Changchun Institute
of Applied Chemistry
Graduate School of the Chinese,
Academy of Sciences
Chinese Academy of Sciences
Changchun, Jilin 130022, China
Fax: (+86) 431-85262656
E-mail: xqu@ciac.jl.cn
Prof. D. Miyoshi, Prof. N. Sugimoto
Frontier Institute for Biomolecular Engineering Research (FIBER)
Konan University
8-9-1 Okamoto, Higashinada-ku, Kobe 658-8501, Japan

DOI: 10.1002/smll.201301273

1. Introduction

Tumor cells are characterized by deregulation of cell cycle-checkpoints, leading to uncontrolled cell division and proliferation under conditions where non-transformed cells cannot enter and pass through the cell cycle. All these may come from over-expression of cyclins and the abnormal activation of cyclin-dependent kinases (CDKs).[1] Cyclins are a super family of proteins whose levels vary in a cyclical fashion during the cell cycle to activate specific CDK required for the proper progression through the cell cycle. Cyclin A_2, a member of cyclin family, is involved in both G1/S and G2/M transitions and participates in DNA replication, transcription and cell cycle regulation.[2] Cumulative evidences support that over-expression of cyclin A_2 contributes to the chromosomal

instability, neoplastic transformation and tumor proliferation.[3] Increased expression of cyclin A_2 has been detected in many types of cancer cells.[4] Therefore, cyclin A_2 can be used as a prognostic indicator in early-stage cancer and served as a promising anticancer target for the development of tumor therapeutic agents.[5] Moreover, its expression level in many types of cancers appears to be of prognostic values such as prediction of aggressiveness, survival or early relapse.[4c,6] Thus, developing a simple, ultrasensitive, selective and inexpensive assay of cyclin A_2 is important for both clinical diagnosis of cancer in the early stage and the treatment.

Currently, protein detection approaches have mainly been dominated by immunological assay methods.[7] However, this technique is limited by the requirement of producing high-quality antibodies, multiple washing steps, and low capacity for multiplexed analyte detection. Recently, in vitro screen techniques produce large number of engineered polypeptide recognition elements that tightly and specifically bind to a wide range of protein targets. The specific peptide and protein interaction provides another molecular recognition for protein sensing, and this strategy eliminates the need for antibodies and has more generality. Based on this novel principle, cyclin A_2 can be detected as low as 0.6 μM using a well-known Tb^{3+} chelating macrocycle modified $p21^{(WAF-1)}$ consensus sequence for a specific cyclin A_2 binding motif (CBM).[8] However, the limited sensitivity of this lanthanide-based sensor remains the significant challenges and makes the assay difficult to use in crude, complex cell extracts and other real samples. The more sensitive assay choosing and non-specific binding (NSB) of incoming target biomolecules preventing are the standard means for promoting efficient cyclin A_2 binding in cell extracts and signal transduction events, as they provide higher sensitivity and specificity.

Electrochemiluminescence (ECL), the smart combination of chemiluminescence and electrochemistry, has become a powerful analytical tool in the detection of biomolecules, clinical diagnostics, environmental and food monitoring, and biowarfare agent detection due to its simplified set-up, label-free, low background signal, and high sensitivity. Since the first report of ECL generated by silicon nanoparticles in 2002,[10] much effort has been devoted to explore the nanomaterials-based new kind of ECL emitters, such as semiconductor nanocrystals or quantum dots(QDs).[11] As finding new luminophors with a high ECL efficiency for bioanalysis is the constant driving force of this area, the family of nanoemitters for ECL has been enlarged from exclusively QDs to other miscellaneous nanomaterials in recent years, with various compositions, sizes and shapes, including metallic nanoclusters,[12] carbon nanodots,[13] metallic oxide semiconductors[14] and even organic nano-aggregates.[15] The advances concerning nanoparticles-based ECL not only open a promising field for the development of new-generation ECL-emitting species, but also promote the development of novel ECL signal-transition platforms for biosensing devices.

Upconversion nanoparticles (UCNPs) have been proposed as a promising new class of biological luminescent labels and as alternatives to conventional labels because of their attractive chemical and optical features, including weak auto fluorescence backgrounds, strong penetration abilities under near-infrared (NIR) radiation, resistance to photobleaching, and low toxicity, etc.[16] Although UCNPs hold great promise in nanotechnology and nanomedicine, their applications in ECL fields still remain unexplored. Our group has firstly reported a facile in situ strategy to fabricate reduced graphene oxide-upconversion hybrid nanomaterials (rGO-UCNPs) ($NaYF_4$: 78 mol% Y^{3+}, 20 mol% Yb^{3+}, 2 mol% Er^{3+}) with amplified ECL performance and characterized this nanomaterials in details.[17] The high intensity and satisfying stability of the ECL signal make the nanomaterials as the superior candidate for further ECL biosensor construction.

2. Results and Discussion

Using ECL as the sensitive detection method, rGO-UCNPs as the novel ECL emitter and a poly (ethylene glycol) (PEG) modified specific hexapeptide P_0 (PEG-RWIMYF) as the recognition probe, we fabricated a cyclin A_2 profiling system in cancer cells. As shown in **Scheme 1**, the specific PEGlyted hexapeptide P_0 was first linked to the rGO-UCNPs modified glassy carbon electrode (GCE) to serve as the detection probe of cyclin A_2 and the prevention agent of NSB simultaneously. The subsequently binding of target cyclin A_2 hindered the access of ECL coreactant ($Na_2S_2O_8$) to the electrode surface, which decreased the ECL signal. P_0, screened from synthetic combinational libraries, is a hexapeptide that binds to a surface pocket in cyclin A_2 with high affinity and inhibits the kinase activity of CDK2-cyclin A complex.[18,19] Meanwhile, as one of the most promising strategies for preparation of anti-biofouling nanomaterials, conjugation of PEG to the materials surface, termed PEGlytion, is often used to prevent the materials from non-specific interactions with biomacromolecules, such as serum components and blood cells.[20] Previous research has already shown that after conjugating antibacterial peptides onto oligo (ethylene glycol) (OEG) brushes, the resultant polymer brushes exhibited

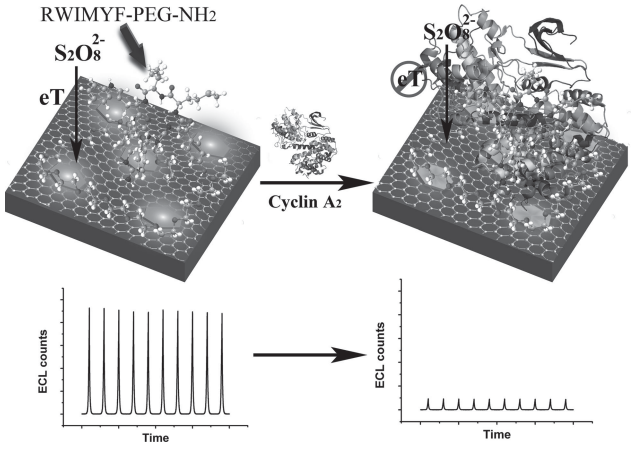

Scheme 1. Schematic illustration of the graphene-upconversion nanocomposite-based peptide sensor for cyclin A_2 detection. It should be noted that the illustration is only a graphic presentation and does not represent the scale of each component and the precise way that PEGlyted P_0 binds onto graphene-upconversion hybrids.

small 2013,
DOI: 10.1002/smll.201301273

NANO MICRO small

both antibacterial and antifouling activity.[21] Inspired by these successful results, here we combined the cyclin A_2 binding hexapeptide P_0 with PEG derivatives to reach the high goal of sensitive and selective detection of cyclin A_2 in cancer cell extracts in the presence of the large amount of other non-specific proteins and biomolecules. The PEGlytion of the peptide probe requires no additional procedure for preventing NSB, which gives a new horizon for electrochemical biosensor fabrication with only one-step modification.

The rGO-UCNPs was synthesized through a one step method directly from graphene oxide by hydrothermal method according to our previous report,[17] in which the fabrication process and characterization of the rGO-UCNPs nanomaterials had been described in details. Meso-tetra(4-carboxyphenyl) porphine (TCPP), a water-soluble porphyrin, was used to functionalize the as-synthesized rGO-UCNPs through ligand exchange of oleic acid-coated UCNPs (OA-UCNPs) with the porphyrin complex TCPP and the non-covalently π–π stacking and hydrophobic forces between TCPP and rGO, as shown in **Figure 1**A.[22,23] The conjugation of TCPP not only permits the dispersion of nanocomposites in water but also introduces abundant carboxylic groups that serve as uniformly distributed sites for following peptide linking while still preserving the excellent conductivity of graphene.[18] Well-defined hexagonal OA-UCNPs nanoparticles with the similar morphology and distinctly enwrapped with gauze-like graphene nanosheets were obtained in the rGO-UCNPs (Figure 1B). The ligand exchange of oleic acid by TCPP did not severely influence the morphology of rGO-UCNPs (Figure 1C) and made the better dispersion of TCPP/rGO-UCNPs hybrids in water (data not shown).

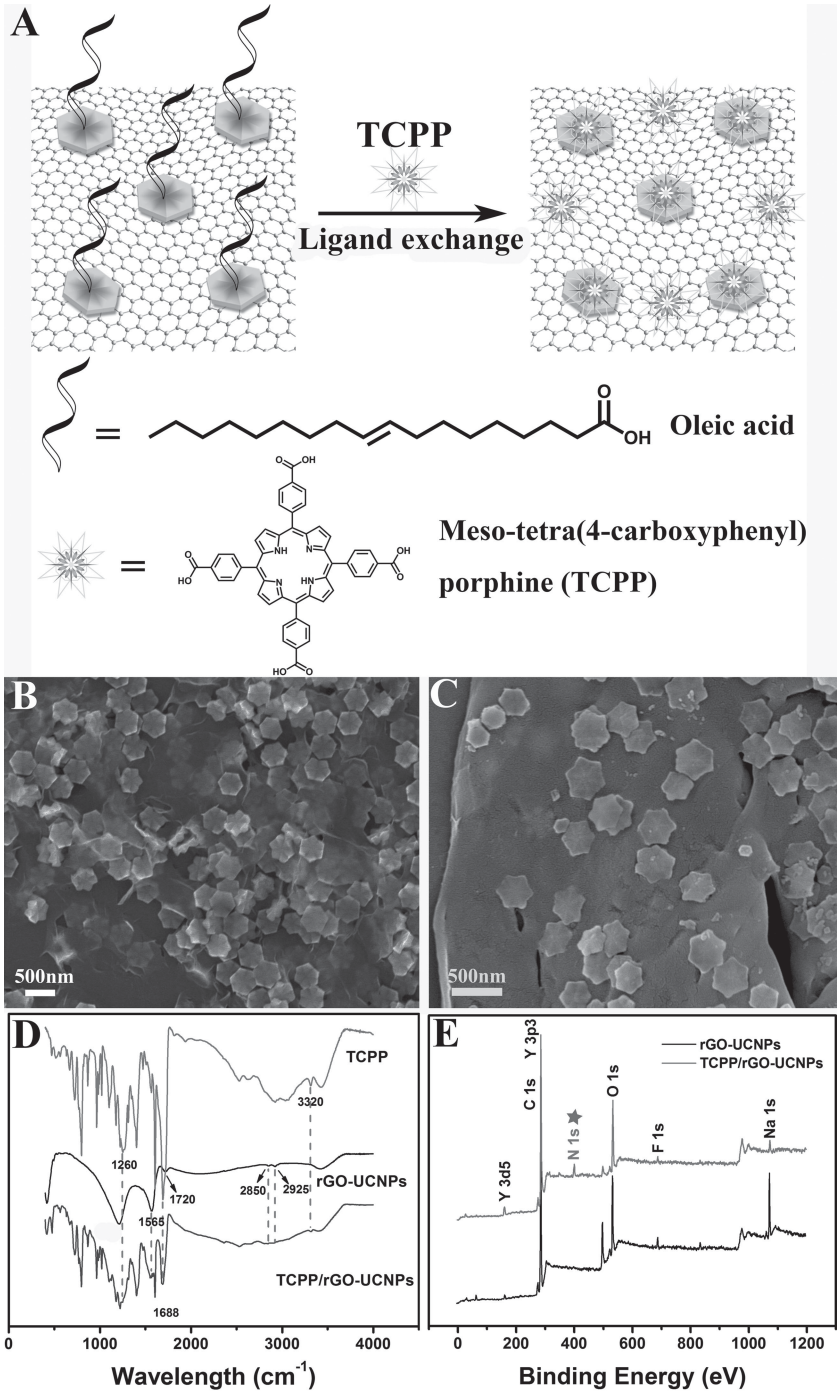

Figure 1. (A) Schematic illustration of synthesis of the porphyrin complex TCPP-modified rGO-UCNPs (TCPP/rGO-UCNPs). Typical SEM images of the synthesized rGO-UCNPs (B) and TCPP/rGO-UCNPs (C). (D) FTIR transmittance spectra of TCPP, rGO-UCNPs and TCPP/rGO-UCNPs. (E) XPS profiles of rGO-UCNPs and TCPP/rGO-UCNPs.

The assembly of the complex TCPP on the surface of the rGO-UCNPs was investigated by FTIR spectrophotometry (Figure 1D). In the FTIR spectra of rGO-UCNPs, the asymmetric bands of the alkyl group at 2850 cm^{-1} and 2925 cm^{-1} corresponded to the C=H stretching vibrations in oleic acid and the band at 1720 cm^{-1} could be assigned to the C=O stretching vibrations from COOH groups of oleic acid.[24] We also observed a band at 1565 cm^{-1} attributed to the skeletal vibration of the graphene sheets in the FTIR spectrum of rGO-UCNPs.[25] In comparison with the spectrum of oleic acid coated rGO-UCNPs hybrids, the bands of the alkyl group at 2850 cm^{-1} and 2925 cm^{-1} disappeared and the new peaks at 1260 cm^{-1}, 1688 $cm^{-1}$and 3320 cm^{-1} attributable to the characteristic feature of stretching band of the amide C–N peak,[26]ν(C=O) vibration in –COOH and N-H groups stretching, respectively, were observed in the FTIR spectrum of TCPP/rGO-UCNPs, suggesting that the complex TCPP had been successfully assembled on the surface of the TCPP/rGO-UCNPs by ligand exchange. Moreover, the presence of the complex

DOI: 10.1002/smll.201301273

TCPP on the surface of the as-prepared TCPP/rGO-UCNPs was also confirmed by X-ray photoelectron spectroscopy (XPS). As shown in Figure 1E, the XPS pattern of nitrogen (N) was observed only for TCPP/rGO-UCNPs and not for oleic acid coated rGO-UCNPs, indicating the presence of TCPP on the surface of as-synthesized TCPP/rGO-UCNPs.[23]

To certify the efficiency of the rGO-UCNPs constructed biosensor for cyclin A_2 analysis, we first investigated the cytotoxity of the nanomaterials and the stability of the nanocomposites modified electrode. MTT results show that the materials possess good biocompatibility (Figure S1 in the Supporting Information), which is necessary before any further potential biomedical applications. Biosensor stability is associated with the reproducibility of the response and depends mainly on the binding force between the modified element and the electrode. As shown in Figure S2 (Supporting Information), TCPP/rGO-UCNPs modified electrode is stable enough without desquamation after hundred rounds of cyclic voltammetry scanning; and also no obvious change of ECL counts is observed for continuous scanning, which indicates that the ECL of the constructed electrode is stable.

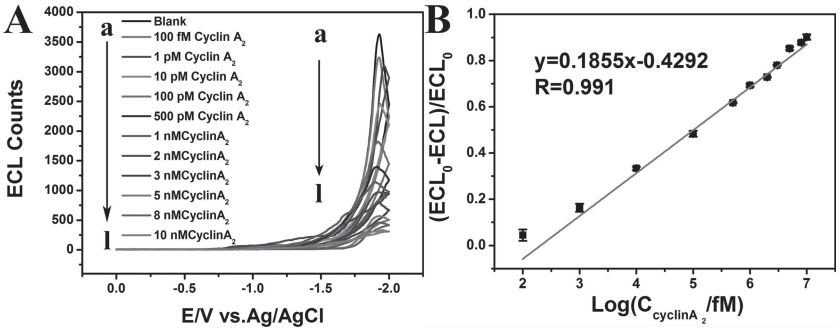

Figure 2. (A) ECL profiles of the TCPP/rGO-UCNPs based biosensor in the absence and presence of different concentrations of cyclin A_2 in pH 7.4 PBS containing 0.1 M $Na_2S_2O_8$. Cyclin A_2 concentration arranged from 100 fM to 10 nM. (B) The calibration curve for cyclin A_2 determination in PBS solution (ECL_0 is the ECL intensity of the peptide modified GCE without target binding). The voltage of the PMT was set at 850 V. Scan rate: 50 mV s^{-1}.

Due to the presence of active $-NH_2$ at the tail end of PEGlyted P_0 peptide probe, P_0 can be linked to the carboxylic groups on TCPP/rGO-UCNPs via a well known carbodiimide-mediated wet-chemistry approach.[18] Figure S3A (Supporting Information) shows a typical cyclic voltammograms (CVs) of $K_3[Fe(CN)_6]$ at different surfaces. A pair of well-defined oxidation and reduction peaks with neglectable attenuation compared to bare glassy carbon electrode (GCE) is observed at the TCPP/rGO-UCNPs modified GCE (TCPP/rGO-UCNPs/GCE), indicating the nanocomposites possess a good conductivity. The immobilization of P_0 on TCPP/rGO-UCNPs/GCE hampers the redox probe $[Fe(CN)_6]^{3-/4-}$ close to the electrode surface and results the slight decrease of redox peak current (Figure S3A in the Supporting Information) and increase of R_{et} value (Figure S3B in supporting information) owing to the dielectric behavior of PEGlyted peptide. Using electrochemical impedance spectroscopy (EIS), a method which is highly suitable for measuring electrode surface changes, we firstly investigate the binding ability of the fabricated biosensor to the target cyclin A_2 (Figure S3B in Supporting Information). The results are consistent with our previous report,[18] indicating the feasibility of this novel ECL platform in cyclin A_2 detection. The amounts of TCPP/rGO-UCNPs used for electrode modification and the concentration of P_0 have been optimized before the ECL sensor applied in cyclin A_2 detection (Figure S4 in the Supporting Information).

According to our previous report,[17] the ECL process of rGO-UCNPs could be expressed as follows:

$$NaYF_4/Yb, Er + e \rightarrow NaYF_4/Yb, Er^{-\bullet} \quad (1)$$

$$S_2O_8^{2-} + e \rightarrow SO_4^{-\bullet} + SO_4^{2-} \quad (2)$$

$$SO_4^{-\bullet} + NaYF_4/Yb, Er^{-\bullet} \rightarrow NaYF_4/Yb, Er^* + SO_4^{2-} \quad (3)$$

$$NaYF_4/Yb, Er^* \rightarrow NaYF_4/Yb, Er + h\nu \quad (4)$$

Once the contact of the coreactant $S_2O_8^{2-}$ to the electrode surface and the interaction between the ECL luminophor and the generated radical ions were prevented, the ECL process was disturbed.[27] Based on the above discussion, the binding of cyclin A_2 to the electrode surface severely decreased the ECL intensity and the intensity depended on the surface coverage of the protein molecules (**Figure 2**A). A semilogarithmic dependence was obtained between the degree of ECL intensity change and cyclin A_2 concentration in the buffer solution, the detection was ranged from 100 fM to 10 nM cyclin A_2 with a correlation coefficient R of 0.991 (Figure 2B). The limit of the detection is calculated to be 10.5 fM (0.52 pg/mL) at 3σ, which is four orders of magnitude lower than the previous reported graphene-based peptide fluorescence assay,[28] and also superior than the recently reported electrochemical impedance spectra method (the calculated detection limit is 0.32 pM).[18] More importantly, the sensitivity of this rGO-UCNPs-based ECL protein detection sensor is superior to the vast majority of the QDs-based ECL biosenor (Table S1 in the Supporting Information). We further tested the selectivity of the novel luminophor TCPP/rGO-UCNPs-based ECL sensor, as shown in **Figure 3**. The sensor showed little response to the non-specific proteins and no apparent attenuation of ECL intensity was observed upon incubation with the non-specific proteins and the starved cell extract which expression level of cyclin A_2 could be neglected.[29] The ultrahigh selectivity of the sensor toward cyclin A_2 can be attributed to the special binding affinity between P_0 and the surface pocket in cyclin A_2.[18,19a,30]

Inspired by the excellent performance of the fabricated ECL sensor in starved cell extracts, we extended our work to detect the expression level of cyclin A_2 in different cancer cells and evaluate the anticancer drug treated cancer cells. The cell culture and cell extracts were prepared as previously

small 2013,
DOI: 10.1002/smll.201301273

NANO MICRO small

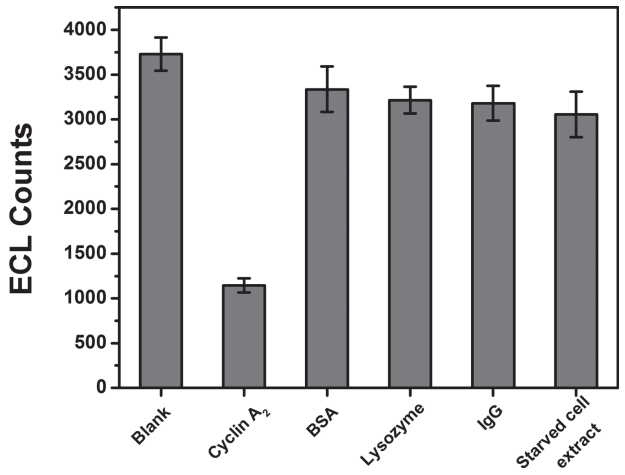

Figure 3. Specificity of the assay for cyclin A_2 based on the decrease of ECL intensity. The concentrations of cyclin A_2 and three non-specific proteins, including BSA, lysozyme and immunoglobulin G (IgG) were 1 nM, [starved cell extract] = 1 mg/mL.

reported.[28,30] The ECL signals of peptide sensor attenuated significantly upon incubation with different concentrations of cyclin A_2 mixed in the starved K562 cell extracts. According to the fitting curve, the detection limit of cyclin A_2 in cell extracts was calculated to be 49.5 fM at 3σ ($R = 0.995$, $n = 3$). As it was reported that cyclin A_2 plays important roles at G_2-M transition and the expression level of cyclin A_2 in G_2-phase was about 11.8 pmol/10.8 g of extracts (it was calculated to be 1.1 pM cyclin A_2 in 1 mg/mL cell extracts) in HeLa cells (human cervical carcinoma cells).[31] The detection limit is lower than the cyclin A_2 expression level, which permits the application of the sensor for the profiling of cyclin A_2 directly in cancer cell extracts. Thus we set out to compare four types of cancer cell lines: K562, HeLa, MDA (human breast carcinoma cell) and MCF-7 (human mammary gland adeno-carcinoma cells) with one normal cell line: HUVEC (human umbilical vein endothelial cells) by measuring the change of ECL signal. As illustrated in **Figure 4**B, the expression level of cyclin A_2 in HeLa cells was in the mid-range in comparation to other cell-lines and K562 cell expressed much higher cyclin A_2 than HeLa cell. The results are consistent with the previous report.[31] While for HUVEC cell extracts, the degree of ECL change was smaller compared to other cancer cell lines under the same experimental conditions, indicating that the sensor developed here could not only detect cyclin A_2 in cell extracts but also differentiate cancer cells from the normal ones. Doxorubicin (DOX), a prominent member of anthracycline antibiotics, has been extensively used for treatment of solid tumors and leukemia. It can lead to cell-cycle arrest at the G_2/M phase and apoptosis.[32] Previous studies demonstrated that cyclin A_2 expression level was significantly up-regulated in anticancer drug DOX-treated K562 cells ($K562^+$).[2e,32] The decrease of the ECL intensity derived from $K562^+$ cells is much higher than that from K562 cells (Figure 4B), which is consistent with the reverse transcriptase-polymerase chain reaction (RT-PCR) and western blotting experiments.[2e] The different responses of TCPP/rGO-UCNPs based ECL sensor between clinical used anticancer drug treated and non-treated cancer cells demonstrated that the sensor can be potentially used for estimating the efficiency to anticancer drugs in cancer therapy.

3. Conclusion

In summary, we have demonstrated that rGO-UCNPs can be used as the new luminophor with a high ECL efficiency and satisfied biocompatibility for bioanalysis. Using TCPP modified rGO-UCNPs and PEGlyted P_0 recognition probe, we fabricated a label-free ECL sensor for cyclin A_2 detection in buffer solution and cell extracts. As a prognostic indicator in early-stage cancer and a promising anticancer target for the development of tumor therapeutic agents, direct profiling the expression level of cyclin A_2 in cancer cells is valuable for both clinical diagnosis of cancer in the early stage and the treatment. Combining the advantages of antifouling PEG with active functional peptide probe for cyclin A_2 recognition and the TCPP/rGO-UCNPs based ultrahigh sensitivity target-signal transition ECL platform, we successfully realized the differentiation of cancer cells from normal ones and the analysis of up-regulated cyclin A_2 expression level in anticancer drug-treated cancer cells. The results demonstrated that the sensor can be potentially used for drug screening, predicting patient prognosis, and also for the evaluation of therapeutic treatments in early-stage cancers. Furthermore, since most of peptide-protein bindings do not produce easily measurable output signal, and this severely hinders homogeneous protein detection. By using graphene-upconversion nanohybrid ECL and peptide as detection probe, the label-free assay reported here represents a new means for simple, economic, ultra sensitive and selective sensing peptide-protein interaction and would shed light on developing of future protein biosensors.

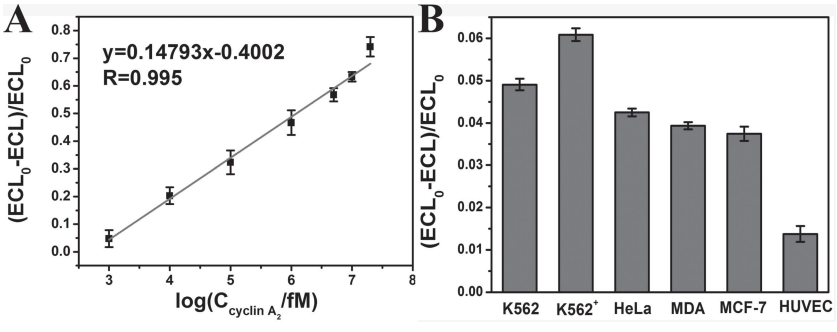

Figure 4. (A) The calibration curve for determination cyclin A_2 suspension in starved K562 cell extracts (1 mg/mL) (ECL_0 is the ECL intensity of the peptide modified GCE treated with only starved K562 cell extracts).(B) Comparison among different cell extracts: K562, DOX-treated K562 ($K562^+$), HeLa, MDA, MCF-7 and HUVEC cells.

4. Experimental Section

Preparations of rGO-UCNPs and TCPP/rGO-UCNPs: The nanocomposites rGO-UCNPs

DOI: 10.1002/smll.201301273

were synthesized according to our previous report.[17] NaOH (1.2 g, 30 mmol), water (6 mL), ethanol (12 mL), and oleic acid (15 mL) were mixed under agitation to form a homogeneous solution. 500 μL of 1.82 mg mL^{-1} GO was added to the homogeneous solution. Then 150 μL, 0.5 M $Ln(NO_3)_3$, (Ln: 78 mol% Y^{3+}, 20 mol% Yb^{3+}, 2 mol% Er^{3+}) aqueous solution was added under magnetic stirring. Subsequently, 1.0 M aqueous NaF (1 mL) solution was added dropwise to the above solution. The mixture was agitated for about 10 min, then transferred to a 50 mL autoclave, sealed, and hydrothermally treated at 200 °C for 8 h. The system was cooled to room-temperature naturally, and the products were deposited at the bottom of the vessel. Pure powders could be obtained by purifying the samples with ethanol several times to remove oleic acid, sodium oleic and other remnants.

TCPP/ rGO-UCNPs were prepared using the ligand-exchange method.[23] Acetonitrile solutions of complex TCPP (2 mmol in total) were added to the prepared rGO-UCNPs (50 mg) in a 10 mL round-bottomed flask. Initially, the nanoparticles were dispersed in the acetonitrileby ultrasonication, and then the mixture was stirred for 1h at room temperature to obtain ahomogeneous phase. Then, the mixture was centrifuged and the collected solid was repeatedly washed with water and acetonitrile. The precipitate could be redispersed in deionized water.

Cell Culture and Cell Extract Preparation: The cell lines: K562 cells, HeLa cells, MCF-7 cells, MDA cells and HUVEC cells were cultured in flasks in Dulbecco's modified Eagle's medium supplemented with 10% fetal bovine serum, penicillin, and streptomycin (100 μg/mL) in an 5% CO_2-humidified chamber at 37 °C. DOX-treated K562 cells were cultured in the medium containing 0.25 μM DOX. The starved, untreated and DOX-treated K562 cells all cultured for 72 h.[2e,2f] The cells were collected and separated from the medium by centrifugation at 3000 rpm for 5 min, then washed twice with a sterile PBS (pH 7.2). Cell lysates were generated by lysing 1×10^7 cells in 500 μL radio immune precipitation assay (RIPA) buffer (PBS containing 1% NP40, 0.5% sodium deoxycholate, 0.1% sodium dodecyl sulphate, 4% aprotinin, 1% sodium orthovanadateand 0.5% PMSF) on ice, centrifuge at 4 °C for 30 min, and discarding the deposition. Protein concentrations were determined using the Bradford assay.

MTT Assay: The toxicity of TCPP/rGO-UCNPs to cells was measured by MTT assay. Briefly, K562 cells were plated at a density of 1×10^4 cells per well in 100 μL of RPMI medium in 96-well plates and grown for 24 h. The cells were then exposed to a series of concentrations of TCPP/rGO-UCNPs composite for 24 h, and the viability of the cells was measured using the methylthiazoletetrazolium method. Controls were cultivated under the same conditions without the addition of the nanocomposites. Then 5 μL of MTT (5 mg/mL) was added into the wells and further incubated for an additional 4 h. Subsequently, the supernatant was discarded, followed by the additional of 100 μL DMSO into each well and incubation in the shaker incubator with gentle shakes. Then the optical density (OD) was read at a wavelength of 570 nm. Relative inhibition of cell growth was expressed as follows: $\% = (1 - [OD]_{test}/[OD]_{control}) \times 100$.

Electrode Modification and ECL Detection of Cyclin A_2: The glassy carbon electrodes (GCE, ϕ = 3 mm, CHI) were polished successively with 1.0, 0.3, and 0.05 μm alumina (Buhler) and sonicated for 3 min before modification. A 10-μL TCPP/rGO-UCNPs solution was dropped on the pretreated GCE and dried at room temperature. The carboxylic groups of TCPP were firstly activated in the activation solution (10 mM EDC and 25mM NHS in MES buffer) for 30 min. After washed by PBS solution, the amino functionalized PEGlyted P_0 was immediately dropped on the TCPP/rGO-UCNPs modified electrode surface and then incubated for 4 h. Unconjugated P_0 was removed by washing the electrode surface with buffer solution. The modified electrodes were stored in air prior to use.

The ECL detection was achieved as following: a 20-μL drop of cyclin A_2 sample at a certain concentration was added onto the fabricated electrodes and incubated at 37 °C for 1 h. After carefully rinsing with PBS toremove the non-captured proteins, the electrodes were used for subsequent assays. The modified electrodes were in contact with 0.1 M PBS (pH 7.4) containing 0.1 M $Na_2S_2O_8$ and scanned from 0 to −2.0 V. The ECL signals related to the different concentrations of cyclin A_2 were measured.

Supporting Information

Supporting information is available from the Wiley Online Library or from the author.

Acknowledgements

This work was supported by 973 Project (2011CB936004, 2012CB720602), and NSFC (21210002, 91213302).

[1] L. H. Hartwell, M. B. Kastan, *Science* **1994**, *266*, 1821.
[2] a) M. Pagano, R. Pepperkok, F. Verde, W. Ansorge, G. Draetta, *Embo J.* **1992**, *11*, 961; b) F. Girard, U. Strausfeld, A. Fernandez, N. J. C. Lamb, *Cell* **1991**, *67*, 1169; c) J. Sobczak-Thepot, F. Harper, Y. Florentin, F. Zindy, C. Brechot, E. Puvion, *Exp. Cell Res.* **1993**, *206*, 43; d) C. F. Lehner, P. H. O'Farrell, *Cell* **1989**, *56*, 957; e) X. Wang, Y. Song, J. Ren, X. Qu, *PLoS One* **2009**, *4*, e6665; f) X. Wang, J. Ren, X. Qu, *ChemMedChem* **2008**, *3*, 940.
[3] a) K. Chi Bui, F. Wu, S. Buckley, L. Wu, R. Williams, D. Carbonaro-Hall, F. L. Hall, D. Warburton, *Am. J. Resp. Cell Mol.* **1993**, *9*, 115; b) C. Liao, S. Q. Li, X. Wang, S. Muhlrad, A. Bjartell, D. J. Wolgemuth, *Int. J. Cancer* **2004**, *108*, 654; c) H. Blegen, N. Einhorn, K. Sjövall, A. Roschke, B. M. Ghadimi, L. M. McShane, B. Nilsson, K. Shah, T. Ried, G. Auer, *Int. J. Gynecol. Cancer* **2000**, *10*, 477.
[4] a) K. Handa, M. Yamakawa, H. Takeda, S. Kimura, T. Takahashi, *Int. J. Cancer* **1999**, *84*, 225; b) P. Paterlini, A. M. Suberville, F. Zindy, J. Melle, M. Sonnier, J. P. Marie, F. Dreyfus, C. Bréchot, *Cancer Res.* **1993**, *53*, 235; c) J. Mrena, J.-P. Wiksten, A. Kokkola, S. Nordling, C. Haglund, A. Ristimaki, *Int. J. Cancer* **2006**, *119*, 1897; d) M. Furihata, T. Ishikawa, A. Inoue, C. Yoshikawa, H. Sonobe, Y. Ohtsuki, K. Araki, S. Ogoshi, *Clin. Cancer Res.* **1996**, *2*, 1781; e) J. Kushner, G. Bradley, B. Young, R. C. K. Jordan, *J. Oral Pathol. Med.* **1999**, *28*, 77.
[5] a) C. McInnes, M. J. I. Andrews, D. I. Zheleva, D. P. Lane, P. M. Fischer, *Curr. Med. Chem.* **2003**, *3*, 57; b) K. L. Ball, S. Lain, R. Fahraeus, C. Smythe, D. P. Lane, *Curr. Biol.* **1997**, *7*, 71; c) N. Mendoza, S. Fong, J. Marsters, H. Koeppen, R. Schwall, D. Wickramasinghe, *Cancer Res.* **2003**, *63*, 1020.

DOI: 10.1002/smll.201301273

[6] a) Y. Chao, Y.-L. Shih, J.-H. Chiu, G.-Y. Chau, W.-Y. Lui, W. K. Yang, S.-D. Lee, T.-S. Huang, *Cancer Res.* **1998**, *58*, 985; b) P. Poikonen, J. Sjostrom, R. M. Amini, K. Villman, J. Ahlgren, C. Blomqvist, *Brit. J. Cancer* **2005**, *93*, 515; c) E. Baldini, A. Camerini, A. Sgambato, T. Prochilo, A. Capodanno, F. Pasqualetti, C. Orlandini, L. Resta, G. Bevilacqua, P. Collecchi, *Anticancer Res.* **2006**, *26*, 4415.
[7] a) C. M. Niemeyer, M. Adler, R. Wacker, *Trends Biotechnol.* **2005**, *23*, 208; b) J. E. Ghadiali, M. M. Stevens, *Adv. Mater.* **2008**, *20*, 4359; c) S. Mao, G. Lu, K. Yu, Z. Bo, J. Chen, *Adv. Mater.* **2010**, *22*, 3521; d) H. J. Lee, D. Nedelkov, R. M. Corn, *Anal. Chem.* **2006**, *78*, 6504.
[8] E. Pazos, D. Torrecilla, M. Vázquez López, L. Castedo, J. L. Mascareñas, A. Vidal, M. E. Vázquez, *J. Am. Chem. Soc.* **2008**, *130*, 9652.
[9] W. Miao, *Chem. Rev.* **2008**, *108*, 2506; b) M. M. Richter, *Chem. Rev.* **2004**, *104*, 3003.
[10] Z. Ding, B. M. Quinn, S. K. Haram, L. E. Pell, B. A. Korgel, A. J. Bard, *Science* **2002**, *296*, 1293.
[11] a) S. Deng, H. Ju, *Analyst* **2013**, *138*, 43; b) Y. Guo, Y. Sun, S. Zhang, *Chem. Commun.* **2011**, *47*, 1595; c) L. Yuan, L. Xu, S. Liu, *Anal. Chem.* **2012**, *84*, 10737.
[12] a) I. Díez, M. Pusa, S. Kulmala, H. Jiang, A. Walther, A. S. Goldmann, A. H. E. Müller, O. Ikkala, R. H. A. Ras, *Angew. Chem. Int. Ed.* **2009**, *48*, 2122; b) L. Li, H. Liu, Y. Shen, J. Zhang, J. Zhu, *Anal. Chem.* **2011**, *83*, 661.
[13] a) L. Zheng, Y. Chi, Y. Dong, J. Lin, B. Wang, *J. Am. Chem. Soc.* **2009**, *131*, 4564; b) L. Wu, J. Wang, J. Ren, W. Li, X. Qu, *Chem. Commun.* **2013**, *49*, 5675.
[14] Z. Lin, Y. Liu, G. Chen, *Electrochem. Commun.* **2008**, *10*, 1629.
[15] W. I. Lee, Y. Bae, A. J. Bard, *J. Am. Chem. Soc.* **2004**, *126*, 8358.
[16] a) F. Wang, X. Liu, *Chem. Soc. Rev.* **2009**, *38*, 976; b) J. Zhou, Z. Liu, F. Li, *Chem. Soc. Rev.* **2012**, *41*, 1323.
[17] M. Yin, L. Wu, Z. Li, J. Ren, X. Qu, *Nanoscale* **2012**, *4*, 400.
[18] L. Feng, L. Wu, J. Wang, J. Ren, D. Miyoshi, N. Sugimoto, X. Qu, *Adv. Mater.* **2012**, *24*, 125.
[19] a) X. Wang, L. Wu, J. Ren, D. Miyoshi, N. Sugimoto, X. Qu, *Biosens. Bioelectron.* **2011**, *26*, 4804; b) N. Canela, M. Orzáez, R. Fucho, F. Mateo, R. Gutierrez, A. Pineda-Lucena, O. Bachs, E. Pérez-Payá, *J. Biol. Chem.* **2006**, *281*, 35942.
[20] a) T. Suma, K. Miyata, Y. Anraku, S. Watanabe, R. J. Christie, H. Takemoto, M. Shioyama, N. Gouda, T. Ishii, N. Nishiyama, K. Kataoka, *ACS Nano* **2012**, *6*, 6693; b) A. Hucknall, S. Rangarajan, A. Chilkoti, *Adv. Mater.* **2009**, *21*, 2441; c) E. Wischerhoff, K. Uhlig, A. Lankenau, H. G. Börner, A. Laschewsky, C. Duschl, J.-F. Lutz, *Angew. Chem. Int. Ed.* **2008**, *47*, 5666.
[21] K. Glinel, A. M. Jonas, T. Jouenne, J. Leprince, L. Galas, W. T. S. Huck, *Bioconjugate Chem.* **2009**, *20*, 71.
[22] L. Wu, J. Wang, L. Feng, J. Ren, W. Wei, X. Qu, *Adv. Mater.* **2012**, *24*, 2447.
[23] Q. Liu, J. Peng, L. Sun, F. Li, *ACS Nano* **2011**, *5*, 8040.
[24] G. Wang, X. Shen, B. Wang, J. Yao, J. Park, *Carbon* **2009**, *47*, 1359.
[25] A. Cao, Z. Liu, S. Chu, M. Wu, Z. Ye, Z. Cai, Y. Chang, S. Wang, Q. Gong, Y. Liu, *Adv. Mater.* **2010**, *22*, 103.
[26] Y. Xu, Z. Liu, X. Zhang, Y. Wang, J. Tian, Y. Huang, Y. Ma, X. Zhang, Y. Chen, *Adv. Mater.* **2009**, *21*, 1275.
[27] G. Jie, J. Zhang, D. Wang, C. Cheng, H.-Y. Chen, J.-J. Zhu, *Anal. Chem.* **2008**, *80*, 4033.
[28] X. Wang, C. Wang, K. Qu, Y. Song, J. Ren, D. Miyoshi, N. Sugimoto, X. Qu, *Adv. Funct. Mater.* **2010**, *20*, 3967.
[29] N. Yeh, J. P. Miller, T. Gaur, T. D. Capellini, J. Nikolich-Zugich, C. de la Hoz, L. Selleri, T. G. Bromage, A. J. van Wijnen, G. S. Stein, J. B. Lian, A. Vidal, A. Koff, *Mol. Cell. Biol.* **2007**, *27*, 5161.
[30] X. Wang, J. Ren, X. Qu, *J. Phys. Chem. B* **2008**, *112*, 8346.
[31] T. Arooz, C. H. Yam, W. Y. Siu, A. Lau, K. K. W. Li, R. Y. C. Poon, *Biochemistry* **2000**, *39*, 9494.
[32] D. A. Gewirtz, *Biochem. Pharmacol.* **1999**, *57*, 727.

Received: April 25, 2013
Revised: June 20, 2013
Published online: